



Allele-Specific Biased Expression of the *CNTN6* Gene in iPS Cell-Derived Neurons from a Patient with Intellectual Disability and 3p26.3 Microduplication Involving the *CNTN6* Gene

Maria M. Gridina¹ · Natalia M. Matveeva¹ · Veniamin S. Fishman^{1,2} · Aleksei G. Menzorov^{1,2} · Helen A. Kizilova¹ · Nikolay A. Beregovoy³ · Igor I. Kovrigin² · Inna E. Pristyazhnyuk¹ · Igor P. Oscorbin⁴ · Maxim L. Filipenko⁴ · Anna A. Kashevarova⁵ · Nikolay A. Skryabin⁵ · Tatyana V. Nikitina⁵ · Elena A. Sazhenova⁵ · Ludmila P. Nazarenko^{5,6} · Igor N. Lebedev^{5,6} · Oleg L. Serov^{1,2}

Received: 22 September 2017 / Accepted: 19 December 2017

© Springer Science+Business Media, LLC, part of Springer Nature 2017

Abstract

Copy number variations (CNVs) of the human *CNTN6* gene caused by megabase-scale microdeletions or microduplications in the 3p26.3 region are often the cause of neurodevelopmental disorders, including intellectual disability and developmental delay. Surprisingly, patients with different copy numbers of this gene display notable overlapping of neuropsychiatric symptoms. The complexity of the study of human neuropathologies is associated with the inaccessibility of brain material. This problem can be overcome through the use of reprogramming technologies that permit the generation of induced pluripotent stem (iPS) cells from fibroblasts and their subsequent in vitro differentiation into neurons. We obtained a set of iPS cell lines derived from a patient carrier of the *CNTN6* gene duplication and from two healthy donors. All iPS cell lines displayed the characteristics of pluripotent cells. Some iPS cell lines derived from the patient and from healthy donors were differentiated in vitro by exogenous expression of the *Ng2* transcription factor or by spontaneous neural differentiation of iPS cells through the neural rosette stage. The obtained neurons showed the characteristics of mature neurons as judged by the presence of neuronal markers and by their electrophysiological characteristics. Analysis of allele-specific expression of the *CNTN6* gene in these neuronal cells by droplet digital PCR demonstrated that the level of expression of the duplicated allele was significantly reduced compared to that of the wild-type allele. Importantly, according to the sequencing data, both copies of the *CNTN6* gene, which were approximately 1 Mb in size, showed no any additional structural rearrangements.

Keywords *CNTN6* gene · 3p26.3 microduplication · Intellectual disability · Induced pluripotent stem cells · in vitro neural differentiation · Allele-specific expression

Introduction

Understanding the molecular bases of the pathogenesis of intellectual disability, autism spectrum disorders (ASD), and other neurodevelopmental disorders in patients with chromosomal rearrangements is complicated by the inaccessibility of neuronal cells for the direct assessment of gene expression profiles. Current achievements in cell reprogramming technology provide a unique method for overcoming this issue by the production of induced pluripotent stem (iPS) cells from the somatic cells of patients with chromosomal disorders. Several reports that demonstrate the value of this approach in modeling well-known chromosomal disorders such as Down syndrome [1, 2] and Turner syndrome [3] have been published. Moreover, subsequent in vitro differentiation of iPS cells into neuronal

✉ Oleg L. Serov
serov@bionet.nsc.ru

¹ Institute of Cytology and Genetics SB RAS, Novosibirsk 630090, Russia

² Novosibirsk State University, Novosibirsk 630090, Russia

³ Institute of Molecular Biology and Biophysics, Novosibirsk 630117, Russia

⁴ Institute of Chemical Biology and Fundamental Medicine SB RAS, Novosibirsk 630090, Russia

⁵ Research Institute of Medical Genetics, Tomsk National Research Medical Center Russian Academy of Sciences, Tomsk 634050, Russia

⁶ Siberian State Medical University, Tomsk 634050, Russia

cells makes it possible to directly assess transcriptional changes in targeted cells with chromosomal aneuploidy [4].

The widespread application of high-resolution array-based comparative genomic hybridization (aCGH) for genetic testing of patients with idiopathic intellectual disability and developmental delay provides a powerful tool for the identification of chromosomal regions associated with cognitive impairment [5]. As a rule, the regions detectable with this method include a few genes or a single gene responsible for a specific phenotype, blurring the border between chromosomal and monogenic diseases [6, 7].

Our attention was attracted to the notable overlapping of neuropsychiatric symptoms in patients carrying either microdeletions or microduplications in the 3p26.3 region [8–13]. For instance, among 3724 individuals tested by aCGH, 14 individuals carrying either deletions (7 patients) or microduplications (7 patients) in this region were identified [11]. Both groups of patients showed various neurodevelopmental disorders, including developmental delays, ASD, seizures, and attention deficit hyperactivity disorder. The 3p26.3 region contains the *CHL1*, *CNTN6*, and *CNTN4* genes, which encode the cell adhesion molecules L1 like, contactin-6 and contactin-4, respectively.

Recently, using the aCGH approach, we studied two patients with neurodevelopmental and neuropsychiatric disorders; one had a microdeletion, and the other had a microduplication involving a single *CNTN6* gene only [14]. Thus, both microdeletions and microduplications of *CNTN6* may be responsible for similar neurodevelopmental or neuropsychiatric phenotypes in spite of the variation in the copy number of the *CNTN6* gene. In addition, some researchers [15, 16] recently suggested that microdeletions and point mutations in the *CNTN6* gene may be associated with autism spectrum disorders and intellectual disability. The protein encoded by this gene is a member of the immunoglobulin superfamily and promotes neurite outgrowth and synaptogenesis, especially in sensorimotor pathways. The *CNTN6* protein is crucial for appropriate orientation of dendrite growth in mouse cortical pyramidal neurons [17] and for synapse formation in the cerebellum [18].

It is important to note that pedigrees with inheritance of 3p26.3 microdeletions and microduplications involving the *CNTN6* gene have been reported in the literature; these pedigrees include families with healthy or mildly affected carriers in several generations [11, 14, 19, 20]. These observations indicate the low penetrance of copy number variations (CNVs) in 3p26.3.

Here, we for the first time report biased allele-specific expression of the *CNTN6* gene in neuronal cells differentiated from iPS cells obtained by reprogramming of skin fibroblasts from a patient with the *CNTN6* microduplication and from two healthy donors with normal karyotype. Surprisingly, we also found that the *CNTN6* gene expression level of the

duplicated allele was significantly reduced in comparison with the normal allele and that its total expression was decreased in neuronal cells.

Materials and Methods

Preparation of Skin Fibroblast Cultures We obtained skin fibroblasts from a previously described patient, K., with intellectual disability and 3p26.3 microduplication of paternal origin [14]. The patient was observed during the European Community's Seventh Framework Program, Project No. 223692 "Improving Diagnosis of Mental Retardation in Children in Eastern Europe and Central Asia through Genetic Characterization and Bioinformatics/Statistics." The project was approved by the Bioethics Committee of the European Parliament. The patient's age at the time of skin biopsy was 13 years. Skin biopsies were also obtained from two healthy donors, S., 31 years of age, and L., 39 years of age. Informed consent for skin biopsy was obtained from the patient, the patient's parents, and the healthy donors.

Cultures of skin fibroblasts were established from the skin biopsies in the following manner: 0.5-cm² pieces of skin from the forearm were washed twice with Hank's solution containing 1% penicillin/streptomycin (Pen Strep, Sigma) and then treated with 0.2% collagenase (Sigma) in culture medium for 3 h at 37 °C. The fibroblast cultures were maintained in DMEM (Gibco) supplemented with 10% fetal bovine serum (Gibco) and 50 mg/ml penicillin/streptomycin (Gibco). The fibroblast culture derived from the patient with 3p26.3 microduplication was designated as TAFdup, and those from the two healthy donors S. and L. were designated as TAF1nor and TAF2nor, respectively.

Generation of iPS Cells from Human Fibroblasts To produce induced pluripotent stem (iPS) cells from the patient's and healthy donors' skin fibroblasts, we used LeGO lentiviral vectors (<http://www.lentigo-vectors.de/vectors.htm>) containing the human reprogramming transcription factors OCT4, SOX2, C-MYC, and KLF4. The lentiviruses were produced in the Phoenix cell line using Lipofectamine 3000 (Invitrogen) according to the manufacturer's recommendations. We used a lentiviral vector carrying the green fluorescent protein (GFP) gene to estimate the multiplicity of infection (MOI); it was 4.6 for TAFdup and more than 10 for TAFnor. Fibroblasts plated on the previous day were transduced with viruses containing the four reprogramming transcription factors in the presence of 5 µg/ml polybrene (Millipore) for 2 days (on the second day, the C-MYC lentivirus was omitted). Until day 10, the culture medium was changed daily with addition of 1 mM valproic acid (Sigma). On day 5, the transduced cells were seeded onto 10-cm culture dishes (2 × 10³ cells per cm²) containing mitomycin C-treated CD-1 mouse embryonic fibroblast feeder cells

in iPS cell medium (DMEM/F12 medium supplemented with 20% KnockOut Serum Replacement, 1% GlutaMAX™-I, 1% MEM NEAA, 1% Pen Strep (all from Gibco), 0.1 mM 2-mercaptoethanol, and 10 ng/ml bFGF (Invitrogen)). On day 18, colonies with iPS cell morphology were picked and expanded. All cell cultures were maintained at 37 °C in an atmosphere of 5% CO₂. The iPS cell clones obtained from TAFdup fibroblasts were designated iTAFdup and iPS cell clones from the fibroblasts TAF1nor and TAF2nor were designated iTAF1nor and iTAF2nor, respectively.

Cytogenetic Analysis of Human Fibroblasts and iPS Cells

Preparation of metaphase chromosomes from human fibroblasts was performed as previously described [21]. Preparation of metaphase chromosomes from iPS cells was performed as previously described with minor modifications [22]. Metaphase plates were analyzed using a Carl Zeiss Axioplan 2 imaging microscope with a CoolCube1 CCD camera, and digital images were analyzed using ISIS 3 (In Situ Imaging System, MetaSystems GmbH) software at the Center for Microscopy of the Institute of Cytology and Genetics.

Isolation of Total DNA from Cell Cultures and Blood Samples

Cultured cells were harvested in 0.25% trypsin solution (Sigma) and washed three times with PBS. Total DNA was isolated by the standard phenol-chloroform extraction method [23] with preliminary treatment with proteinase K (20 mg/ml, SibEnzyme) for 3–4 h.

Whole blood from the patient and from the healthy donors, as well as from their parents and grandparents, was collected in 9-ml tubes (BD Vacutainer Systems). Total DNA was isolated by the standard phenol-chloroform extraction method.

Microsatellite Analysis To determine the parental origin of chromosome 3, PCR analysis of the polymorphic microsatellite D3S1768 was performed using the primers forward 5′-GGT TGC TGC CAA AGA TTA GA-3′ and reverse 5′-CAC TGT GAT TTG CTG TTG GA-3′. PCR was performed for 30 cycles at an annealing temperature of 55 °C. Electrophoresis was performed in 4% agarose gels in TRIS-EDTA-acetate buffer.

Whole-Genome Sequencing of TAFdup Fibroblasts Genomic DNA was extracted from primary TAFdup fibroblasts at passages 10–11 and subjected to paired-end Illumina sequencing, generating approximately 750 million reads. The reads were aligned to the hg19 human genome and processed using the algorithms MANTA [24], CANVAS [25], and SVDetect [26] to detect structural variations. In addition, all 23 *CNTN6* gene exons of TAFdup fibroblasts were sequenced. Primer-BLAST software was used to design primers for all 23 exons of the *CNTN6* gene (Table 1) [27–29]; the PCR conditions are described above. DNA sequencing of PCR products was

performed using the BigDye® Terminator v3.1 kit (Thermo Fisher Scientific) on an Applied Biosystems 3500 Genetic Analyzer according to the manufacturer's recommendations.

Generation and Histological Analysis of Teratomas For teratoma formation, SCID mice were used. All animal studies were undertaken with prior approval from the Interinstitutional Bioethical Committee at the Institute of Cytology and Genetics. Teratomas were produced by injection of iPS cell clumps (passages 9–13) into the shin of the hind leg [30]. Teratomas were dissected after 6–12 weeks, fixed in Bouin solution and embedded in paraffin according to standard histological protocols. The paraffin sections were stained with hematoxylin-eosin. Images were analyzed on a Carl Zeiss Axioscop 2+ microscope with an AxioCam HRc CCD camera. Digital images were obtained using AxioVision software.

Ngn2-Induced Differentiation of iPS Cells to iN Cells For differentiation of iPS cells into neuronal cells, we used a protocol in which induced neuronal (iN) cell generation is induced by a single transcription factor, neurogenin-2 (*Ngn2*) [31]. Three lentiviral constructs (FUW-TRE *Ngn2*/Puro containing full-length mouse *Ngn2* and the puromycin-resistance genes, M2RtTA and FUW-TRE EGFP containing the *GFP*) were used to generate iN cells from iPS cells. The lentiviruses were produced in the Phoenix cell line using Lipofectamine 3000 (Invitrogen) according to the manufacturer's recommendations. Co-transfection of the respective lentiviral vector pDNA and three helper plasmids (pRSV-REV, pMDLg/pRRE, and pCMV-VSVG) was used to produce each of the three viruses.

Prior to differentiation, iPS cells (passages 10–17) were maintained without feeder cells on Matrigel hESC-Qualified Matrix (Corning). iPS cells were disaggregated using TrypLE™ Express (Gibco) and seeded on Matrigel-coated wells of 6-well plates (3×10^5 cells per well) in mTeSR™1 medium (STEMCELL Technologies) containing 10 μM ROCK inhibitor Y27632 (Abcam). The day after seeding, the cells were transduced with lentiviruses in culture medium containing 5 μg/ml polybrene (Millipore). MOI was estimated by flow cytometry using a BD FACSAria. We used the lentiviruses at MOIs greater than 10 to produce iN cells. To induce *Ngn2* gene expression in the transduced iPS cells, 2 μg/ml doxycycline (DOX; Sigma-Aldrich) was added 1 day after transduction in medium consisting of DMEM/F12, 1% MEM NEAA, 1% Pen Strep, 1% N2 supplement, human BDNF (10 ng/ml) (all from Gibco), mouse laminin (0.2 μg/ml, Sigma), and human NT-3 (10 ng/ml, PeproTech). *Ngn2*-expressing cells were selected with puromycin (1 μg/ml, Gibco) the day after DOX induction. To ensure that the initial conditions of differentiation were uniform for each iPS cell clone, equal numbers of iPS cells (45×10^3 cells/cm²) were plated on mitomycin C-treated mouse glia after 1 day of

Table 1 List of primers

Name of primers	Forward primer sequence 5'–3'	Reverse primer sequence 5'–3'
CNTN6_exon1	AATGCAGTGAAACCAGAGGAA	TTCTCATTGCAGCAGACACAG
CNTN6_exon2	TCGTGTTGTACGTTTTTCATTTCA	CACCCATAGAAAAGAAATACAATGCC
CNTN6_exon3	TAGACTTGCATTCAAAACAGGGC	GTGCCACAGGTAGGATTTT
CNTN6_exon4	TTGCAGGAATTAGAACTACATGTTT	ATTGGAGCTTTGCCTTCCGA
CNTN6_exon5	AATCTGCTTTTCTTTGTTTTCCAAG	CACTCTCCAAGTGACCGCAT
CNTN6_exon6	CAGATATGAATGAATGCAGTAAGGA	GGCTCCACAAAACAAGAAGG
CNTN6_exon7	CTCCAGAAATGCTGCTAGCTCT	GGCCTGGTCATTGTCTCAGT
CNTN6_exon8	ACCGTCTTCTATTCTAATGAGGTG	CCCGTGACACTTTTTTACAACA
CNTN6_exon9	TCCTTCTGATCTCTACAGCCCT	CTCCATTAACATTAGCTGTTTCTGT
CNTN6_exon10	ACAAGCATCTTTATATGCCTTTTCC	ACGTCATTTTGAATTTGTTGGTTGT
CNTN6_exon11	TAGCATAGCAAGTCACCCCTG	AGAGGAAATTTTGAAAGGCCTACTA
CNTN6_exon12	ACCAGTGTGAAGAGCCTTACT	ACAGGTTTGACACCATAACACA
CNTN6_exon13	ACCATAGGCTAGCATTTTATAAGC	CCATGCAAATAAAGATGGAGAGAGT
CNTN6_exon14	TCCATTTCTCCCTTTCTGTCTGC	TGGTGTGGTTTCTCAGAGGT
CNTN6_exon15	ACTTCTAAGCACAAACAGGTAA	TGACCCAAAACACTTTTGTCACT
CNTN6_exon16	CCCAACCTAGGTGCCTTAGTG	ACGAAATCTTCCACACTTTTAGAAC
CNTN6_exon17	TGCCATCCCACATTTCTCTTG	TCTGGCCAGTTAAATCTCTTTTCT
CNTN6_exon18	GTGATTGATCACATTCTGCCCA	TGGAACAAGGGAACACAAACT
CNTN6_exon19	AGTTTGTGTTCCCTTGTTCCTA	AGGAGCTATTGCGAAGTCCA
CNTN6_exon20	TCCTTGTGGTTGTGGTTGAT	AGCAAAGGAATAGGTTGCTCT
CNTN6_exon21	TGCATCATACTTTGACCATGAGC	GGGTGTCACATGTTTCATTCTCT
CNTN6_exon22	TCCAGAACAGTTGTGTGAACCTT	GAATTTTCATGCTGCAGCTGTCT
CNTN6_exon23	GTCCTTGACAAAAGACACGGT	ACAGCAGTTACAACCTCCCCAG
FOXP1	GTGCATAGCTCTTTACCTGTG	CCTGAACTGAAGGGCTCTGTG
BRN2	CATTCCCCTTACGAGGGTGT	TTGCCTTCGATAAAGCGGGT
CUX1	CTCACACAAAACGTGGATG	CCGCTCTATTCTCACGCAT
CUX2	GCCTACCTGAAACGTGCGTA	TGACGGTGTGGTCTTGAGG
SYN1	CCCAAATACCAGGCAACCCA	GGAAGGGGCTCAACAGTAGG
vGLUT1	ATTACTCGTCCCGCCATTC	TGCTGGTAGGGGAGATGTGA
vGLUT2	GGGGAAGAGGCATTTTGCTTG	CCAACCACCCAAAACAGCTAC
FEZF2	CGATGACTGGCAGCAAACCTC	TTCGCTTGTACAGGAGGATTTAC
BHLHE22	AAGCCTGGAGAGTGTGTTGAATG	ATGCTACCCAAACCCTAACCC
GAPDH	GTGGACCTGACCTGCCGTCT	GGAGGAGTGGGTGTCGCTGT

puromycin selection. From this day until the end of the differentiation period, the cells were cultured in Neurobasal Medium containing 2% B27 supplement, 1% GlutaMAX™-I, 1% Pen Strep, human BDNF (10 ng/ml) (all from Gibco), and NT-3 (10 ng/ml, PeproTech). The cells were differentiated for 3 weeks; then, total RNA was extracted from the obtained iN cells and used for droplet digital PCR analysis, see below.

Neuronal Differentiation of iPS Cells through the Neural Rosette Stage Spontaneous neuronal differentiation of iPS cells was induced by embryoid body (EB) formation as described by Muratore et al. [32]. Briefly, iPS cells (passages 10–17) were maintained without feeder cells in mTeSR1 medium (STEMCELL Technologies) on Matrigel hESC-Qualified Matrix (Corning). EBs were formed from iPS

cells in hanging drops during a 2-day incubation. Subsequently, the EBs were transferred to low-adherence dishes for 5 days in neuronal induction medium (DMEM/F12, 1% GlutaMAX™-I, 1% MEM NEAA, 1% Pen Strep, 1% N2 supplement (all from Gibco), and 2 µg/ml heparin (Sigma)). The EBs were then transferred to poly-L-ornithine/laminin-coated (Sigma) wells of six-well plates (10 EBs per well) to form neural rosettes. Neural rosettes were manually picked and plated on poly-L-ornithine/laminin-coated wells in neuronal induction medium supplemented with EGF (20 ng/ml, Invitrogen) and bFGF (20 ng/ml, Invitrogen). Neural progenitor cells (NPCs) were passaged every 4 days with 0.5 µM EDTA. NPCs were induced to differentiate into post-mitotic neurons by withdrawing bFGF and EGF; the cells were then placed on

N2B27 medium consisting of a 1:1 mixture of DMEM/F12 and Neurobasal Medium supplemented with 1% GlutaMAX™-I, 1% Pen Strep, 0.5% N2 supplement, 1% B27 supplement, human BDNF (10 ng/ml) (all from Gibco), mouse laminin (0.2 µg/ml, Sigma), and 200 µM L-ascorbic acid (Sigma). The medium was replaced every other day. The total time of neuronal differentiation of iPS cells by this protocol is approximately 40 days.

Isolation of Mouse Glial Cells Cultures of mouse glial cells were obtained from the forebrains of 2–3 days CD-1 mice according to the protocol described by Vierbuchen et al. [33]. Glial cells were passaged three times to remove neurons before co-culture with iN cells.

Immunofluorescence Staining Immunofluorescence staining of iPS cells was performed as previously described [34] using the following primary antibodies: Nanog (rabbit, 1:200; Abcam, catalog ab21603), Oct4 (rabbit, 1:200; Abcam, catalog ab19857), TRA-1-60 (mouse, 1:250; Abcam, catalog ab16288), and SSEA4 (mouse, 1:200; Abcam, catalog ab16287). Immunofluorescence staining of iN cells was performed with the following primary antibodies: Tubb3 (mouse, 1:500; Covance, catalog MMS-435P), NF 200 (rabbit, 1:200; Sigma-Aldrich, catalog N4142), MAP2 (rabbit, 1:500; Abcam, catalog ab32454), synaptophysin (mouse, 1:1000; BioLegend, catalog MMS-618R), and PSD95 (rabbit, 1:1000; Abcam, catalog ab18258). Anti-rabbit and anti-mouse IgG antibodies conjugated with Alexa Fluor 546 (1:500; Invitrogen, catalog A-11010 and A-11060, respectively) were used as the secondary antibodies. Neuronal markers of mature neurons were analyzed after 21–25 days of *Ngn2*-induced differentiation of iPS cells. Images were analyzed on an Axio Imager M2 fluorescence microscope (Carl Zeiss).

RT-PCR Analyses The expression of neuronal markers was examined in iN cells after 21–25 days of *Ngn2*-induced differentiation of iPS cells. Total cellular RNA was extracted from iN cells using TRI Reagent (Sigma-Aldrich) according to the manufacturer's instructions. The concentration and purity of the RNA were assessed by measuring the optical density of the RNA solution at 260 and 280 nm using a NanoDrop (Thermo Scientific). The RNA was treated with DNase I (Thermo Fisher Scientific) to remove trace amounts of genomic DNA, and 0.6 µg of total RNA was used to generate cDNA using RevertAid RT Kit (Thermo Fisher Scientific) according to the manufacturer's instructions. The primer sequences are shown in Table 1.

Droplet Digital PCR Analysis Total RNA was prepared as described above. Droplet Digital PCR (ddPCR) was performed using a QX100 system (Bio-Rad) according to the manufacturer's recommendations. The reactions (20 µl volume)

contained 1× ddPCR™ Supermix for Probes (no dUTP), 900 nM primers, and 250 nM probes and template. The primers and probes sequences are shown in Table 2. ddPCR reactions for each sample were performed in duplicate. The droplets were generated using DG8™ cartridges and transferred to PCR plates. PCR was conducted according to the following program: 95 °C for 10 min, then 45 cycles of 95 °C for 30 s and 60 °C for 1 min. All steps had a ramp rate of 2 °C per second. The droplets were read in a droplet reader, and the results were analyzed using Quanta Soft software (Bio-Rad). Thresholds were set to define the positive and negative droplets, and the data were exported as a comma-separated values (CSV) file. ddPCR was performed for three independent biological replicates. *ACTB* was chosen as a reference gene. The absolute number of cDNA copies of *CNTN6* was derived from ddPCR and normalized to the number of cDNA copies of *ACTB*.

Electrophysiological Analysis of iN Cells The electrophysiological analysis of iN cells was performed after 22 and 45 days of *Ngn2*-induced differentiation of iPS cells. Patch clamp recordings were performed for GFP-positive iN cells. The whole-cell configuration of the patch clamp technique was used to record voltage-gated transmembrane currents and action potentials. The patch pipettes were pulled from standard borosilicate glass pipettes 1.5 mm in outer diameter (Sutter Instruments, USA; puller PC-10, Narishige) and had a resistance of 6–10 MΩ. Under whole-cell voltage clamp conditions, the membrane voltage was held at –70 mV. For the registration voltage-gated currents, voltage steps from –80 to +10 mV at 10-mV intervals were used. The duration of each step was 100 ms, and each step was preceded by hyperpolarization to –90 mV for 300 ms to remove current inactivation. Test pulses of 100-ms duration were applied every 2 s. Action potentials were elicited by injection of 100-ms depolarizing currents with graded stimulus amplitudes under current clamp conditions. Standard external solution contained 150 mM NaCl, 5 mM KCl, 1 mM CaCl₂, 2 mM MgCl₂, 10 mM HEPES-pH 7.4 (pH adjusted with NaOH), and 10 mM glucose. The patch pipette solution contained 136.5 mM K-glucuronate, 17.5 mM KCl, 9 mM NaCl, 1 mM MgCl₂, 10 mM HEPES, and 0.2 mM EGTA (pH 7.2). All experiments were performed at room temperature (20–22 °C).

Cells were visualized with a fluorescence microscope Axio Examiner.A1 microscope (Carl Zeiss, Germany) equipped with the appropriate filter sets. Digital pictures of the recorded cells were acquired using a digital camera (AxioCam, Carl Zeiss). Single-cell patch clamp recordings were performed using an EPC 10 USB amplifier (HEKA Elektronik) filtered below 2.9 kHz using a Bessel low-pass filter. The data were sampled and analyzed using PatchMaster software (HEKA Elektronik) and Igor Pro software (Wavemetrics).

Table 2 List of primers and probes for ddPCR

Name of primers and probes	Primer sequence 5'–3'	Probe sequence 5'–3'
ACTB	Forward TCGTGCCTGACATTAAGGAG Reverse CTTCTCCAGGGAGGAGCTG	HEX-CGCCCTGGACTTCGAGCAAGAGA-BHQ
CNTN6	Forward CCAAGTGAACCATCAGAATTGTAA Reverse CCGACTTCTCCACCTCCAT	HEX-AGCATCAGTCCCTGTTGTGGCACC-BHQ
CNTN6_exon6_nor	Forward GGACCTTCAATGATAACCCCTTA Reverse GTTCCCGTCTCTTGAGATACAA	FAM-CGTCCAAGAGGACAATAGGCG-BHQ HEX-CGTCCAAGAGGAAAATAGGCG-BHQ
CNTN6_exon18_nor	CAGTGGGCTCGACAACCT AGACAGTGGGATGATGCTTTCATT	FAM-CCAAGGAGAAAGTATCATCTGTGG-BHQ HEX-CCAAGGAGAAAGTGTCTATCTGTGG-BHQ
CNTN6_exon6_dup	Forward GGACAATAGGCGATTGTATCTC Reverse CCCACATCTGATGGTTCCAC	HEX-AGACGGGAAACTTGTACATTGCC-BHQ FAM-AGACGGGAAACCTGTACATTGCC-BHQ
CNTN6_exon18_dup	Forward CAACCTGGTCCAAGGAGAAAAG Reverse CAAAGGGAGACAGTGGGATGA	FAM-AGGTTTGTCTACAGAAATGAAAGC-BHQ HEX-AGGTTTGTCTACAGAAATGAAAGC-BHQ

Results

Characterization of the CNTN6 Gene Microduplication The TAFdup fibroblasts derived from the patient with a *CNTN6* gene duplication had the normal karyotype 46,XY (Fig. 1a). According to the pedigree, the patient inherited the microduplication from the father [14]. Figure 1 illustrates the presence of both parental alleles of the D3S1768 microsatellite in the nine subclones derived from single cells of primary TAFdup fibroblasts (Fig. 1c). The results did not indicate any signs of mosaicism among the TAFdup fibroblasts with respect to the presence of the microduplication of *CNTN6*.

Genomic DNA extracted from the TAFdup fibroblasts at passages 10–11 was subjected to whole-genome sequencing. The sequence data were analyzed using the MANTA, CANVAS, and SVDetect algorithms to search for structural variations within the 3p26.3 region containing the *CNTN6* gene. All algorithms produced similar results indicating that the size of the microduplication was approximately 1 Mb: MANTA—560,685–1,504,677 bp; CANVAS—662,227–1,504,619 bp; and SVDetect—560,671–1,504,741 bp (GRCh37/hg19 human genome reference) and that the microduplication begins approximately 600 kb upstream of the *CNTN6* gene and ends more than 50 kb downstream of its stop codon. Figure 1e illustrates the result of sequencing of the border between the first and the second *CNTN6* gene copies. The first copy ends at 1,504,678 bp, and the second copy began at 560,685 bp. This suggests that the DNA fragment from 560,685 to 1,504,678 bp was duplicated in patient K.

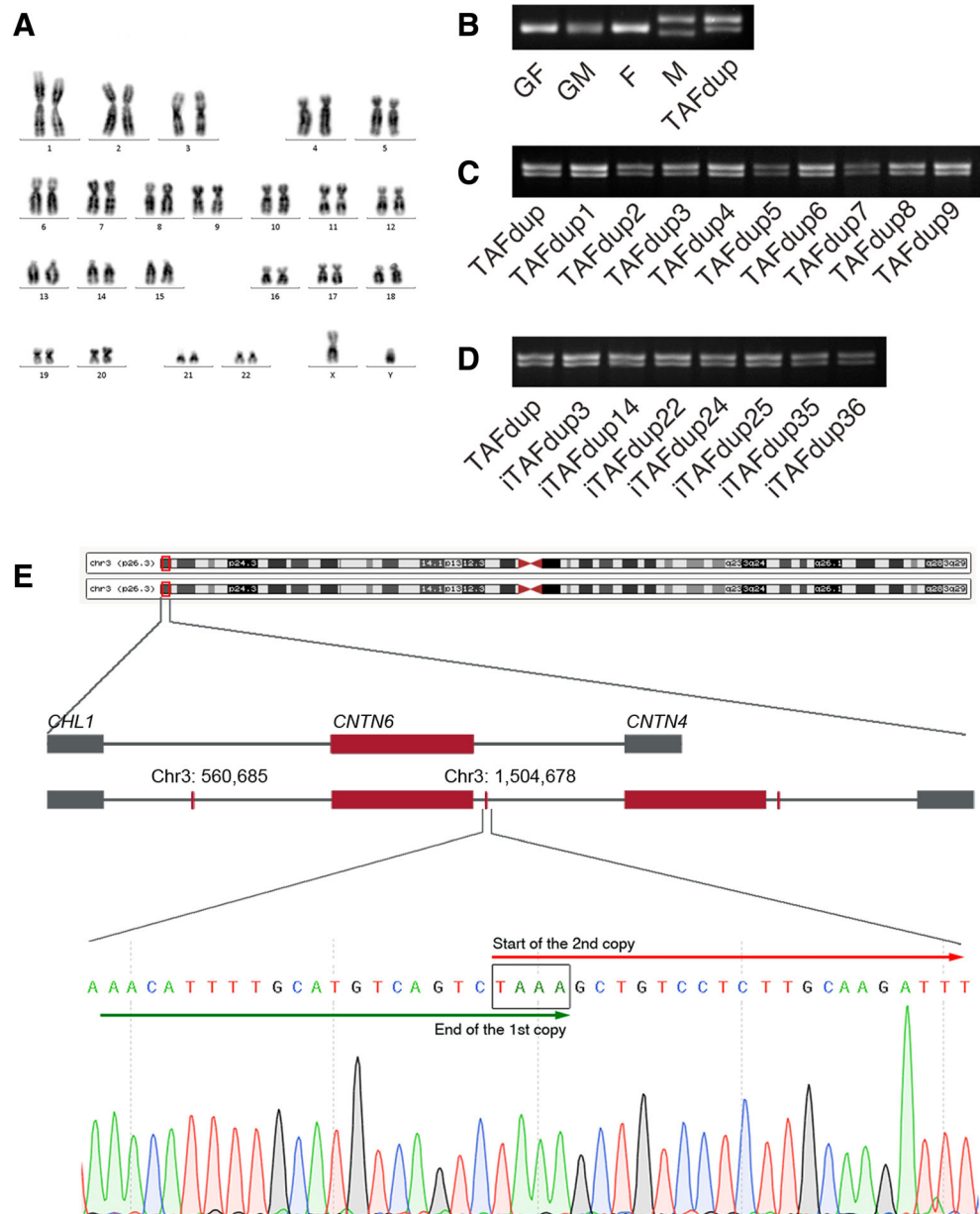
In addition, we checked the aligned reads in the Integrative Genomics Viewer (<http://software.broadinstitute.org/software/igv/>) and were able to identify sequences spanning the duplicated segment in TAFdup cells from nucleotides 560,685 to 1,504,666 in the 3p26.3 region. Importantly, none of the software analyses revealed additional rearrangements affecting the *CNTN6* gene with the

exception of a small microduplication approximately 500 bp in length identified within intron 2; this microduplication was detected by MANTA but not by CANVAS or SVDetect. Furthermore, the presence of this presumed 500-bp microduplication was not confirmed by direct sequencing of the chromosome 3 (1,216,883–1,217,448 bp). Here, it is pertinent to note that, with the exception of some SNPs, sequencing of all 23 *CNTN6* exons of the TAFdup fibroblasts did not reveal any differences between the duplicated and wild-type alleles of the *CNTN6* gene. The sequencing data did not reveal any structural variations either within the *CNTN6* gene or in the region surrounding the gene in the TAFdup fibroblasts.

We identified the following SNPs of the *CNTN6* gene exons in TAFdup fibroblasts: rs150338565 (T/C, exon 6, chr3:1,295,687, GRCh38/hg38; T marks the paternal duplicated *CNTN6* allele), rs4684146 (C/T, exon 18, chr3:1,383,061, GRCh38/hg38; C marks the paternal duplicated *CNTN6* allele), and rs2291101 (G/A, exon 18, chr3:1,383,034, GRCh38/hg38). We also sequenced the *CNTN6* exon 6 of TAF1nor and TAF2nor fibroblasts derived from two healthy men. We found rs2291101 (G/A, exon 18, chr3:1,383,034, GRCh38/hg38) in TAF2nor fibroblasts and a new SNP in TAF1nor fibroblasts (C/A, exon 6, chr3:1,295,653, GRCh38/hg38). This SNP leads to the substitution of glutamic acid for aspartic acid; because both of these residues are polar and negatively charged, it is unlikely that this variation affects the structure of the encoded protein. In addition, we sequenced exon 6 of the *CNTN6* gene from blood sample DNA obtained from the healthy parents of the TAF1nor and TAF2nor fibroblast donors. This allowed us to establish the parental origin of the alleles: **A** marks the maternal *CNTN6* allele, **C** marks the paternal allele in TAF1nor, **G** marks the maternal allele, and **A** marks the paternal allele in TAF2nor.

Generation and Characterization of iPS Cells Obtained from TAFdup, TAF1nor, and TAF2nor Fibroblasts We used Yamanaka's transcription factors cocktail containing OCT4,

Fig. 1 **a** Karyotype 46,XY of a TAFdup fibroblast derived from a patient carrying the duplication of *CNTN6* gene. **b** Analysis of the D3S1768 microsatellite marking parental chromosome 3 in the patient with a duplication of *CNTN6* gene (TAFdup) and his grandfather (GF), grandmother (GM), father (F), and mother (M). The slow-migrating variant in the patient is seen to be inherited from the mother. **c** Presence of both parental variants of the D3S1768 microsatellite in primary TAFdup fibroblasts and their 9 subclones from TAFdup1 to TAFdup9, each of which originated from a single cell. **d** Presence of the parental variants of the D3S1768 microsatellite in 7 clones of the iTAFdup series from iTAFdup3 to iTAFdup36, each of which were derived from single cells of TAFdup. **e** Schematic representation of 3p26.3 in normal (upper) and duplicated (lower) alleles and extension of the duplication junctions. Sequence analysis of the duplication junctions in a patient carrying the duplication of *CNTN6* gene



SOX2, C-MYC, and KLF4 to reprogram human fibroblasts into iPS cells. We produced 7 iPS cell clones from TAFdup fibroblasts, 12 iPS cell clones from TAF1nor fibroblasts, and 7 iPS cell clones from TAF2nor.

Cytogenetic analysis of the iTAFdup, iTAF1nor, and iTAF2nor cell clones showed that they had the normal karyotype 46,XY (Fig. 2a). Nevertheless, chromosome mosaicism often arises during the generation and cultivation of iPS cells [35, 36]. We performed microsatellite analysis of the iTAFdup clones and observed both parental D3S1768 microsatellite variants marking the parental chromosome 3 (Fig. 1d), i.e., there were no signs of mosaicism among the iTAFdup clones with respect to the presence or absence of chromosome 3 carrying the *CNTN6* duplication.

All iPS cell clones had typical human embryonic stem (ES) cell morphology. Most of the cells were positive for key markers of pluripotent cells such as OCT4 and NANOG and for the surface antigens TRA-1-60 and SSEA4 (Fig. 2b–f).

Teratomas produced from the iTAFdup, iTAF1nor, and iTAF2nor clones contained derivatives of the three embryonic layers: ectoderm, endoderm, and mesoderm. These data indicate that the iTAFdup, iTAF1nor, and iTAF2nor cell clones are pluripotent. Based on histological analysis of the teratomas, we selected the iTAFdup14, iTAFdup22, and iTAFdup24 clones carrying the *CNTN6* duplication for neuronal differentiation.

Characterization of iN Cells Derived from iTAFdup and iTAFnor Cells iN cells were produced from two iTAF1nor

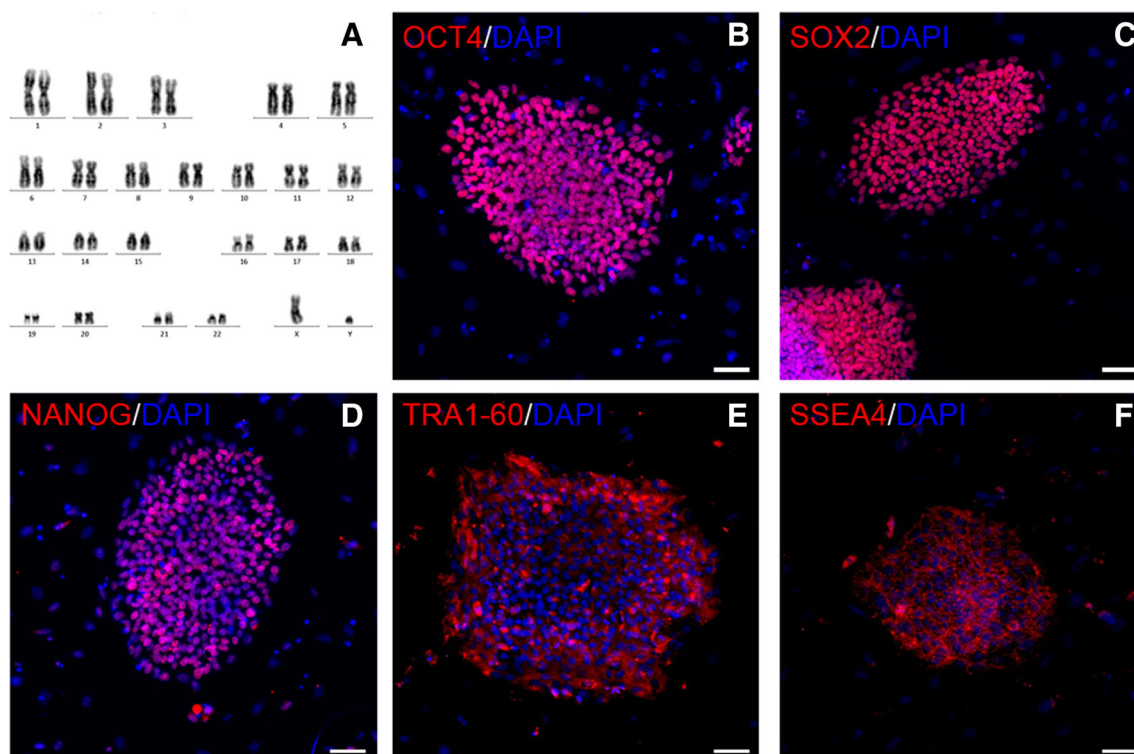


Fig. 2 Characterization of human iPS cells. **a** A karyotype 46,XY of an iTAFdup22 cell. **b–f** Immunofluorescence analysis of pluripotency markers using antibodies against OCT4 (**b**), SOX2 (**c**), NANOG (**d**),

TRA1–60 (**e**), and SSEA4 (**f**) in clones of iPS cells of the iTAFdup and iTAF1nor series. Most iPS cells are positive for these markers. Scale bars 20 μ m

and three iTAFdup iPS cell clones by forced expression of the transcription factor *Ngn2* [31]. After 10–14 days of induced differentiation, most cells displayed extensive neurite outgrowth and formed a dense network (Fig. 3a). More than 90% of the differentiated cells obtained from the iTAF1nor and iTAFdup iPS cell clones were positive for beta-tubulin. In addition, immunofluorescent staining showed that most of the iN cells derived from iTAF1nor and iTAFdup were positive for MAP2 and NF200 (Fig. 3b) after 24 days of differentiation. Moreover, there were neurons enriched in puncta after staining with antibodies against the synapse-associated proteins PSD95 and synaptophysin (Fig. 3b).

We also evaluated the expression of some neural markers of iN cells by RT-PCR. After 3 weeks of differentiation, we observed the expression of a broad range of neuronal markers in *Ngn2*-induced neurons derived from both iTAF1nor and iTAFdup cells. These markers included the telencephalic markers *FOXP1* and *BRN2*, the layer II-III neuronal markers *CUX1* and *CUX2*, and synaptic proteins such as *SYN1*, vesicular glutamate transporter 1, and vesicular glutamate transporter 2. Moreover, *FEZF2*, which is highly expressed in layer 5 pyramidal cells, was also detected (Fig. 3c).

Electrophysiological Properties of iN Cells To functionally characterize the mature iN cells, we examined their electrophysiological properties using the patch clamp technique.

Electrophysiological measurements were performed on GFP-positive cells with clear neuronal morphology after 22 and 40 days of differentiation.

Neurons differentiated from both iTAF1nor and iTAFdup clones displayed similar ability to fire action potentials (APs) in response to depolarizing current pulses (Fig. 3d(i)). During whole-cell recording in voltage-clamp mode, iN cells derived from iTAF1nor and iTAFdup exhibited rapidly inactivating inward current with a rise time of few milliseconds followed by outward currents, corresponding to the opening of voltage-dependent Na⁺ and K⁺ channels. The inward current was completely blocked by inclusion of tetrodotoxin in the external solution (Fig. 3(ii)). Thus, iN cells obtained from the healthy donors and from the patient with the duplicated *CNTN6* gene appear to exhibit functional membrane properties and activities characteristic of neurons.

Total CNTN6 Gene Expression in *Ngn2*-Induced Neurons RT-PCR analysis revealed that the expression of *CNTN6* was activated on the second day of *Ngn2*-induced differentiation (Fig. 4a). We used a highly sensitive and accurate ddPCR method to follow the dynamics of *CNTN6* expression in iN cells. iTAF1nor25 was subjected to neural differentiation for 2, 7, 10, 15, and 21 days. The amount of *CNTN6* transcripts increased during the differentiation period (Fig. 4b).

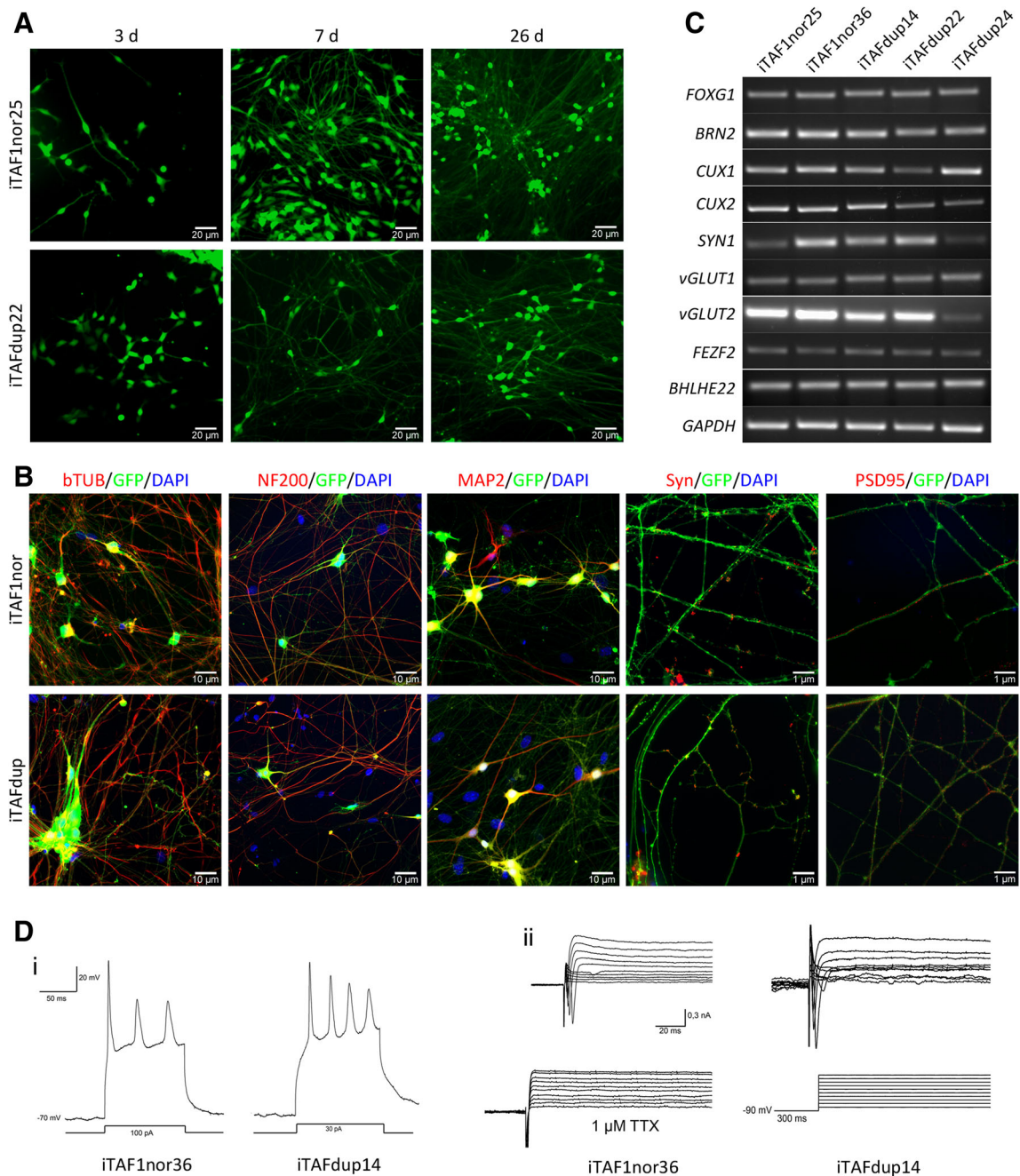


Fig. 3 *Ngn2*-induced neuronal differentiation of human iPS cells. **a** GFP images of live *Ngn2*-induced iPS cells at various time points (**d**) showing that both iTAF1nor and iTAFdup cells quickly acquire neuronal morphology. **b** At 3 weeks, iN cells obtained from both iTAF1nor and iTAFdup cells expressed the neuronal markers (red) beta-tubulin, MAP2, NF200, PSD95, and synaptophysin. The markers were identified by immunofluorescence using specific antibodies. Nuclei were stained with DAPI (blue). **c** RT-PCR analysis of *FOXG1*, *BRN2*, *CUX1*, *CUX2*, *SYN1*, *vGLUT1*, *vGLUT2*, *FEZF2*, *BHLHE22*, and *GAPDH* (internal control) gene expression in iN cells from two iTAF1nor and three

iTAFdup clones. **d** Electrophysiological properties of iN cells after 40 days of differentiation from iTAF1nor and iTAFdup clones. *i* Action potentials were observed; representative voltage responses of iN cells to currents of 100 and 30 pA are shown. *ii* Voltage clamp recording in iN cells shows putative voltage-gated Na⁺ (inward) and K⁺ (outward) currents. For the initiation of voltage-gated currents, voltage steps from -80 to +10 mV at 10-mV intervals were used. The holding potential was -70 mV. The inward currents were completely blocked by 1 μM tetrodotoxin, indicating that they were Na⁺-driven

To compare the level of *CNTN6* gene expression in iN cells obtained from healthy donors with that in iN cells from the patient with the duplicated *CNTN6* gene, two iTAF1nor clones (iTAF1nor25 and iTAF1nor36), one iTAF2nor5 clone,

and three iTAFdup clones (iTAFdup14, iTAFdup22, and iTAFdup24) were subjected to neuronal differentiation by forced expression of exogenous *Ngn2*. The results of quantitative measurements of the *CNTN6* gene expression in these

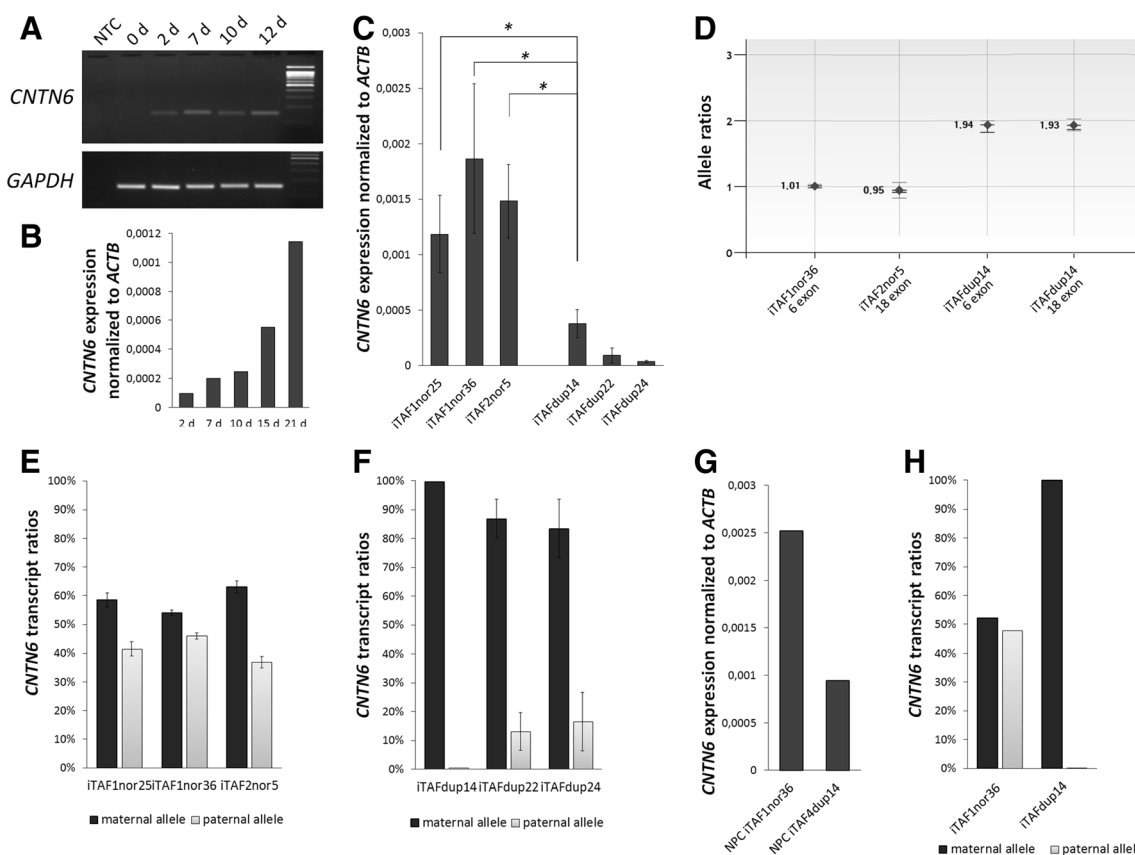


Fig. 4 Analysis of *CNTN6* gene expression in iN cells obtained by in vitro neuronal differentiation of human iPS cells. **a** RT-PCR analysis of *CNTN6* in iTAF1nor25 iN cells at various time points (days). *GAPDH* was used as an internal control. **b** Dynamics of *CNTN6* expression during *Ngn2*-induced neuronal differentiation of iTAF1nor25. *CNTN6* gene expression was normalized to that of *ACTB*. **c** Comparison of the *CNTN6* transcript levels in iN cells from healthy donors (iTAF1nor25, iTAF1nor36, and iTAF2nor5) with those in iN cells from the patient with the duplicated *CNTN6* gene (iTAFdup14, iTAFdup22, and iTAFdup24) at 3 weeks of differentiation. *CNTN6* gene expression was normalized to that of *ACTB*. The data are presented as the mean \pm SD ($*p < 0.05$, Student's *t* test). **d** *CNTN6* allele ratios estimated by ddPCR for iPS cells from healthy donors (iTAF1nor36 and iTAF2nor5) and from the

patient with a *CNTN6* duplication (iTAFdup14). **e** Ratios of *CNTN6* allele transcripts in iN cells generated by the *Ngn2*-induced neuronal differentiation of iTAF1nor25, iTAF1nor36, and iTAF2nor5. The data are presented as the mean \pm SD. **f** Ratios of *CNTN6* allele transcripts in iN cells generated by *Ngn2*-induced neuronal differentiation of three iTAFdup clones carrying a microduplication within the *CNTN6* gene. Despite the interclonal variability, excess of expression of the maternal allele over the paternal allele is clearly observed. The data are presented as the mean \pm SD. **g** Expression of the *CNTN6* gene in NPC-derived neuronal cells generated by spontaneous differentiation of iTAF1nor36 and iTAFdup14 via EBs. **h** Ratios of *CNTN6* allele transcripts in NPC-derived neuronal cells generated by spontaneous differentiation of iTAF1nor36 and iTAFdup14 via EBs

clones, based on three replications, are presented in Fig. 4c. It is important to note that there is statistically significant variability in the expression of *CNTN6* between iN cells derived from iTAFdup14 and those derived from the iTAFdup22 and iTAFdup24 clones, whereas the differences in *CNTN6* expression between iN cells derived from the latter two clones are statistically insignificant. The variability in the expression of *CNTN6* between iN cells derived from the iTAF1nor25, the iTAF1nor36, and iTAF2nor5 clones is statistically insignificant. In spite of the interclonal variability in the expression of *CNTN6* within each series, Fig. 4a shows that in iN cells derived from both iTAF1nor and iTAF2nor5 clones expression of the *CNTN6* gene is several fold higher than that in iN cells derived from the iTAFdup clones. The minimal expression level of *CNTN6* observed in iN cells derived from iTAFdup24 is 2–3% of

that from the iTAFnor clones, and the maximal expression level of *CNTN6* in iTAFdup14 iN cells is approximately 20–30% of that in the iTAFnor iN cells. These interclonal differences in expression of the *CNTN6* in iN cells derived from iTAFnor and iTAFdup clones are statistically significant.

Allele-Specific *CNTN6* Expression in *Ngn2*-Induced Neurons

Because we found significantly reduced expression of the *CNTN6* gene in iTAFdup neurons compared with expression in iN cells derived from iTAF1nor and iTAF2nor, it was important to determine whether there is a difference in the expression levels of the normal and duplicated *CNTN6* alleles. To address this issue, we used TaqMan probes to distinguish SNPs from the parental alleles of *CNTN6* for the iTAF1nor, iTAF2nor and iTAFdup clones.

To ensure that the probes and primer sets used in this study allowed us to accurately distinguish the parental alleles, we analyzed the allele ratios in genomic DNA (gDNA). gDNA from iTAF1nor36, iTAF2nor5 and iTAFdup14 was digested by HindIII (5 U, SibEnzyme) directly in the Bio-Rad® Droplet Digital SuperMix prior to droplet generation. ddPCR analysis of iTAF1nor36 and iTAF2nor5 gDNA yielded *CNTN6* allele ratios of 1.01 and 0.95, respectively. Analysis of iTAFdup14 gDNA gave *CNTN6* allele ratios of 1.94 for exon 6 and 1.93 for exon 18 (Fig. 4d). These results are consistent with the aCGH data [14] and allowed us to use the designed probes to quantify *CNTN6* transcripts from parental alleles.

We analyzed allele-specific *CNTN6* expression in iN cells derived from the iTAF1nor25, iTAF1nor36, and iTAF2nor5 clones in three independent replicas. Figure 4e shows the statistically significant differences in the ratios of the maternal and paternal allele transcripts of the *CNTN6* gene; the ratios were 58.5 to 41.5% for iTAF1nor25, 54 to 46% for iTAF1nor36, and 63.1 to 36.9% for iTAF2nor5. Thus, the data indicate that expression of the maternal allele was slightly higher than expression of the paternal allele in neurons obtained from the analyzed clones.

Analysis of allele-specific *CNTN6* expression was performed for iN cells originating from iTAFdup14, iTAFdup22, and iTAFdup24 using probes that distinguish the SNPs in exon 6 of the parental alleles. The results of quantitative measurements obtained in three independent experiments are shown in Fig. 4f. The duplicated allele of the *CNTN6* gene is expressed at a level many times lower than the level of expression of the normal allele: in the iTAFdup14 clone, less than 0.5% of the total expression was represented by the paternal allele versus 99.5% of the maternal; in iTAFdup22 and iTAFdup24, these values were 13 versus 87% and 16.5 versus 83.5%, respectively. The differences are statistically significant. It is important to emphasize that the same allele-specific expression bias was revealed through the use of probes distinguishing SNPs in exon 18 of the *CNTN6* gene.

Allele-Specific *CNTN6* Expression in NPC-Derived Neurons To exclude a possible influence of the differentiation strategy on allele-specific *CNTN6* expression, we used another protocol [32] to obtain post-mitotic neurons derived from iTAF1nor36 and iTAFdup14 cells. After 8 weeks of differentiation, neurons derived from NPC were positive for beta-tubulin and MAP2. Figure 4g illustrates that total expression of the *CNTN6* gene is more abundant in iTAF1nor36 than in iTAFdup14 NPC-derived neurons. Moreover, the expression of the maternal allele is slightly higher than that of the paternal allele in iTAF1nor36-derived neurons and many times higher than that of the paternal allele in iTAFdup14-derived neurons (Fig. 4h). The extremely low expression (approximately 0.1%) of the paternal allele of the *CNTN6* gene in iTAFdup14 NPC-derived neurons compared to that of the

maternal allele resembles that in iN cells derived from the clone. These data are in good agreement with the results obtained by allele-specific expression analysis of the *CNTN6* gene in iN cells derived from iTAFdup and iTAF1nor cells.

Discussion

In a previous study, a 766.1-kb microduplication of 3p26.3 region involving the *CNTN6* gene was detected by an Agilent 60K array in patient K, who displays developmental, speech and language delays, abnormal skull shape, and facial dysmorphism [14]. According to our genome sequencing of fibroblasts derived from this patient, the duplicated segment is located between nucleotides 560,685 and 1,504,678 in the 3p26.3 region; hence, its size is approximately 1 Mb. It is important to note that the duplicated segment, which begins approximately 600 kb upstream of the *CNTN6* gene and ends more than 50 kb downstream of its stop codon, does not show any structural variations either inside the *CNTN6* gene or in the region surrounding the gene. In addition, subcloning of primary fibroblasts obtained from the patient indicated that the population is represented by cells carrying both parental chromosomes 3 based on microsatellite analysis.

To determine the effect of the microduplication in the *CNTN6* gene on its expression in neurons, we chose a two-step approach to the in vitro generation of neural cells; the first step involved the production of iPS cells from fibroblasts, and the second step was either neural differentiation of the iPS cells under forced expression of the transcription factor *Ngn2* or spontaneous differentiation of iPS cells into neural cells via EBs. iPS cells obtained from a patient carrying the microduplication of the *CNTN6* gene and iPS cells obtained from two healthy donors showed similar pluripotent characteristics; they were positive for typical markers of pluripotent cells such as OCT4, NANOG, TRA-1-60, and SSEA4 and displayed the ability to generate teratomas containing derivatives of three embryonal layers and the ability to form EBs. In addition, microsatellite analysis revealed that no loss of the duplicated allele of the *CNTN6* gene had occurred during the generation of the iPS cell clones.

We chose a protocol based on the forced expression of the transcription factor *Ngn2* to induce neural differentiation of iPS cells [31] for two reasons; *Ngn2* converts human iPS cells into functional neurons with nearly 100% yield and purity after puromycin selection, and the neurons obtained in this way express markers that are characteristic of layer II-III excitatory cortical neurons. In fact, we observed the appearance of cells with neuronal morphology that were positive for beta-tubulin in less than 10–12 days by forced expression of *Ngn2*. After 21–24 days of *Ngn2*-induced differentiation, the neurons acquired mature pre- and postsynaptic specializations (positive for MAP2, NF200, and the synapse-associated proteins PSD95

and synaptophysin), and after 40 days they displayed electrophysiological activities characteristic of mature neurons. Moreover, in addition to the telencephalic markers FOXG1, BRN2, CUX1, and CUX2, which are characteristic of neurons in cortical layers II–III as described by Zhang et al. [31], we identified FEZF2, which is characteristic of layer V pyramidal cells, in our experiments. The presence of neuronal markers characteristic of pyramidal cells is important because the gene product of *CNTN6*, together with other contactins, plays important roles in brain development during the critical phase of establishing brain systems and their plasticity via neurite outgrowth, synaptogenesis, and terminal branching of axons to form neural circuits [37, 38]. It is important to note that iN cells obtained from iPS cells derived from healthy donors and those derived from a patient carrying a microduplication within the *CNTN6* gene had similar characteristics with respect to markers and electrophysiological activities.

We used another technology to generate neural cells from iPS cells via NPC. It provides a broader spectrum of neural derivatives, including neurons, astrocytes, and oligodendroglia [39–42]. We also observed these types of cells after differentiation iPS cells using a protocol developed by Muratore et al. [32].

The main aim of this study was the quantitative estimation of *CNTN6* expression in in vitro-generated neurons derived from iPS cells obtained from healthy donors and from a patient carrying a microduplication of the *CNTN6* gene. The total expression of the *CNTN6* in iN cells derived from iPS cells from healthy donors was severalfold in excess of that in iN cells derived from iPS cells carrying the microduplication. The observed differences in total *CNTN6* expression in neurons originating from iPS cells that carry the gene duplication may be due to the effect(s) of this duplication.

The variability in total *CNTN6* expression among iN cells from different iPS cell clones derived from the patient with the *CNTN6* duplication and iN cells from iPS cells from healthy donors deserves special attention. In fact, minimal expression of *CNTN6* was observed in iTAFdup24 (2–3% compared with iTAF1nor clones), intermediate expression was found in iTAFdup22 (10–14% compared with iTAF1nor clones), and maximal expression was observed in iTAFdup14 (20–30% compared with iTAF1nor clones). This interclonal variability was highly reproducible.

The significant decrease in total *CNTN6* expression in iN cells with the *CNTN6* duplication compared with those derived from healthy donors can be explained by a dramatic decrease in expression of the paternal inherited duplicated allele compared with the wild-type allele. In spite of interclonal variability in the expression of the paternal duplicated allele, its level of expression was significantly lower than that of the normal allele. Importantly, minimal expression

of the paternal allele was observed in the iTAFdup14 iN cells, and similar low expression of the allele was also found in neural cells obtained via NPC technology. It is pertinent to note that the maternal allele of the *CNTN6* gene was expressed at a slightly higher level than the paternal allele in iN cells derived from iPS cells from healthy donors. The revealed interclonal variability of the allelic expression of *CNTN6* in iN cells is reminiscent of the phenomenon of random monoallelic expression (RME), which is manifested during in vitro formation of neural progenitor cells (NPC) from mouse embryonic stem cells (ESC) [43]. Those researchers described variability in the monoallelic expression of many autosomal loci in NPC clones derived from ESC. The use of an independent approach based on sequencing technology indicated that 2.5–5% of autosomal genes are expressed by RME [44–46]. However, in our case, the variability in allelic *CNTN6* expression was most clearly manifested in iN cells carrying the duplicated *CNTN6*, whereas in iN cells containing two wild-type alleles, this variability was slight. An undefined dependence on parental inheritance in the manifestation of the mutant phenotype associated with deletion of the *CNTN6* gene was noted earlier in a study of family pedigrees [20]; however, there are no data on imprinting in this region of human chromosome 3.

In any case, our data suggest that dramatically reduced expression of two copies of the duplicated *CNTN6* allele compared with the wild-type allele may underlie the neurodevelopmental and neuropsychiatric anomalies observed in the patient carrying this microduplication. Moreover, our data help to explain the presence of similar clinical symptoms in a patient carrying a deletion of the *CNTN6* gene and a patient carrying a microduplication of this gene [14].

Acknowledgements The LeGO lentiviral vectors containing the human reprogramming transcription factors OCT4, SOX2, C-MYC, and KLF4 were kindly provided to us by Dr. Sergej L. Kiselev (Moscow). Three lentiviral constructs (FUW-TRE Ngn2/Puro, containing full-length mouse *Ngn2* and puromycin-resistance genes, and M2RfTA and FUW-TRE EGFP, containing the *GFP* gene) were kindly provided to us by Dr. Thomas Südhof (Stanford, CA, USA). Patient's fibroblasts samples were obtained from the collection «Biobank of populations of Northern Eurasia» financed by the Federal Agency for Scientific Organizations of Russia Federation program for supporting the bioresource collections in 2017 (project no. 0550-2017-0019). We thank the family of the patient with 3p26.3 microduplication for their collaboration. We are grateful to the donors of skin fibroblasts and to their parents for their voluntary participation in the research. Cell culture was performed at the Collective Center of ICG SB RAS "Collection of Pluripotent Human and Mammalian Cell Cultures for Biological and Biomedical Research" (state project No. 0324-2016-0002 of Russian Academy of Sciences).

Funding This study was supported by the Russian Science Foundation, grant no. 14-15-00772.

References

- Mou X, Wu Y, Cao H, Meng Q, Wang Q, Sun C, Hu S, Ma Y et al (2012) Generation of disease-specific induced pluripotent stem cells from patients with different karyotypes of Down syndrome. *Stem Cell Res Ther* 3(2):14. <https://doi.org/10.1186/scrt105>
- Hibaoui Y, Feki A (2015) Concise review: methods and cell types used to generate Down syndrome induced pluripotent stem cells. *J Clin Med* 4(4):696–714. <https://doi.org/10.3390/jcm4040696>
- Luo Y, Zhu D, Du R, Gong Y, Xie C, Xu X, Fan Y, Yu B, Sun X, Chen Y (2015) Uniparental disomy of the entire X chromosome in Turner syndrome patient-specific induced pluripotent stem cells. *Cell Discovery*, 1, Article number: 15022.
- Hibaoui Y, Grad I, Letourneau A, Sailani MR, Dahoun S, Santori FA, Gimelli S, Guipponi M et al (2014) Modelling and rescuing neurodevelopmental defect of Down syndrome using induced pluripotent stem cells from monozygotic twins discordant for trisomy 21. *EMBO Mol Med* 6(2):259–277. <https://doi.org/10.1002/emmm.201302848>
- Vissers LE, Gilissen C, Veltman JA (2016) Genetic studies in intellectual disability and related disorders. *Nat Rev Genet* 17(1):9–18. <https://doi.org/10.1038/nrg3999>
- Mikhail FM, Lose EJ, Robin NH, Descartes MD, Rutledge KD, Rutledge SL, Korf BR, Carroll AJ (2011) Clinically relevant single gene or intragenic deletions encompassing critical neurodevelopmental genes in patients with developmental delay, mental retardation, and/or autism spectrum disorders. *Am J Med Genet A* 155A(10):2386–2396. <https://doi.org/10.1002/ajmg.a.34177>
- Kasnauskienė J, Ciuladaite Z, Preiksaitienė E, Utkus A, Peculyte A, Kučinskis V (2013) A new single gene deletion on 2q34: *ERBB4* is associated with intellectual disability. *Am J Med Genet A* 161A(6):1487–1490. <https://doi.org/10.1002/ajmg.a.35911>
- Shoukier M, Fuchs S, Schwaibold E, Lingen M, Gärtner J, Brockmann K, Zim B (2013) Microduplication of 3p26.3 in non-syndromic intellectual disability indicates an important role of *CHL1* for normal cognitive function. *Neuropediatrics* 44(05):268–271. <https://doi.org/10.1055/s-0033-1333874>
- Te Weehi L, Maikoo R, Mc Cormack A, Mazzaschi R, Ashton F, Zhang L, George AM, Love DR (2014) Microduplication of 3p26.3 implicated in cognitive development. *Case Rep Genet* 2014:295359.
- Palumbo O, Fischetto R, Palumbo P, Nicastro F, Papadia F, Zelante L, Carella M (2015) *De novo* microduplication of *CHL1* in a patient with non-syndromic developmental phenotypes. *Mol Cytogenet* 8(1):66. <https://doi.org/10.1186/s13039-015-0170-3>
- Hu J, Liao J, Sathanoori M, Kochmar S, Sebastian J, Yatsenko SA, Surti U (2015) *CNTN6* copy number variations in 14 patients: a possible candidate gene for neurodevelopmental and neuropsychiatric disorders. *J Neurodev Disord* 7(1):26. <https://doi.org/10.1186/s11689-015-9122-9>
- Li C, Liu C, Zhou B, Hu C, Xu X (2016) Novel microduplication of *CHL1* gene in a patient with autism spectrum disorder: a case report and a brief literature review. *Mol Cytogenet* 9(1):51. <https://doi.org/10.1186/s13039-016-0261-9>
- Huang AY, Yu D, Davis LK, Sul JH, Tsetsos F, Ramensky V, Zelaya I, Ramos EM et al (2017) Rare copy number variants in *NRXN1* and *CNTN6* increase risk for Tourette syndrome. *Neuron* 94(6):1101–1111. <https://doi.org/10.1016/j.neuron.2017.06.010>
- Kashevarova AA, Nazarenko LP, Schultz-Pedersen S, Skryabin NA, Salyukova OA, Chechetkina NN, Tolmacheva EN, Rudko AA et al (2014) Single gene microdeletions and microduplication of 3p26.3 in three unrelated families: *CNTN6* as a new candidate gene for intellectual disability. *Mol Cytogenet* 7(1):97. <https://doi.org/10.1186/s13039-014-0097-0>
- Lin YC, Frei JA, Kilander MB, Shen W, Blatt GJ (2016) A subset of autism-associated genes regulate the structural stability of neurons. *Front Cell Neurosci* 10:263–268
- Mercati O, Huguet G, Danckaert A, André-Leroux G, Maruani A, Bellinzoni M, Rolland T, Gouder L et al (2017) *CNTN6* mutations are risk factors for abnormal auditory sensory perception in autism spectrum disorders. *Mol Psychiatry* 22(4):625–633. <https://doi.org/10.1038/mp.2016.61>
- Ye H, Tan YL, Ponniah S, Takeda Y, Wang SQ, Schachner M, Watanabe K, Pallen CJ et al (2008) Neural recognition molecules *CHL1* and *NB-3* regulate apical dendrite orientation in the neocortex via PTP alpha. *EMBO J* 27(1):188–200. <https://doi.org/10.1038/sj.emboj.7601939>
- Sakurai K, Toyoshima M, Ueda H, Matsubara K, Takeda Y, Karagogeos D, Shimoda Y, Watanabe K (2009) Contribution of the neural cell recognition molecule *NB-3* to synapse formation between parallel fibers and Purkinje cells in mouse. *Dev Neurobiol* 69(12):811–824. <https://doi.org/10.1002/dneu.20742>
- Van Esch H, Backx L, Pijkels E, Fryns JP (2009) Congenital diaphragmatic hernia is part of the new 15q24 microdeletion syndrome. *Eur J Med Genet* 52(2-3):153–156. <https://doi.org/10.1016/j.ejmg.2009.02.003>
- Moghadas S, van Haeringen A, Langendonck L, Gijsbers ACJ, Ruivenkamp CAL (2014) A terminal 3p26.3 deletion is not associated with dysmorphic features and intellectual disability in a four-generation family. *Am J Med Genet A* 164A(11):2863–2868. <https://doi.org/10.1002/ajmg.a.36700>
- Kruglova AA, Kizilova EA, Zhelezova AI, Gridina MM, Golubitsa AN, Serov OL (2008) Embryonic stem cell/fibroblast hybrid cells with near-tetraploid karyotype provide high yield of chimeras. *Cell Tissue Res* 334(3):371–380. <https://doi.org/10.1007/s00441-008-0702-9>
- Prokhorovich MA, Lagarkova MA, Shilov AG, Karamysheva TV, Kiselyov SL, Rubtsov NB (2007) Cultures of hESM human embryonic stem cells: chromosomal aberrations and karyotype stability. *Bull Exp Biol Med* 144(1):126–129. <https://doi.org/10.1007/s10517-007-0271-z>
- Current protocols in human genetics/editorial board, Nicholas C. Dracopoli et al. 1994. V. 1: 4.6.6.
- Chen X, Schulz-Trieglaff O, Shaw R, Barnes B, Schlesinger F, Källberg M, Cox AJ, Kruglyak S et al (2016) Manta: rapid detection of structural variants and indels for germline and cancer sequencing applications. *Bioinformatics* 32(8):1220–1222. <https://doi.org/10.1093/bioinformatics/btv710>
- Roller E, Ivakhno S, Lee S, Royce T, Tanner S (2016) Canvas: versatile and scalable detection of copy number variants. *Bioinformatics* 32(15):2375–2377. <https://doi.org/10.1093/bioinformatics/btw163>
- Zeitouni B, Boeva V, Janoueix-Lerosey I, Loeillet S, Legoix-né P, Nicolas A, Delattre O, Barillot E (2010) SVDetect: a tool to identify genomic structural variations from paired-end and mate-pair sequencing data. *Bioinformatics* 26(15):1895–1896. <https://doi.org/10.1093/bioinformatics/btq293>
- Koressaar T, Remm M (2007) Enhancements and modifications of primer design program Primer3. *Bioinformatics* 23(10):1289–1291. <https://doi.org/10.1093/bioinformatics/btm091>
- Untergasser A, Cutcutache I, Koressaar T, Ye J, Faircloth BC, Remm M, Rozen SG (2012) Primer3—new capabilities and interfaces. *Nucleic Acids Res* 40(15):e115. <https://doi.org/10.1093/nar/gks596>

29. Ye J, Coulouris G, Zaretskaya I, Cutcutache I, Rozen S, Madden T (2012) Primer-BLAST: a tool to design target-specific primers for polymerase chain reaction. *BMC Bioinformatics* 13(1):134. <https://doi.org/10.1186/1471-2105-13-134>
30. Hentze H, Soong PL, Wang ST, Phillips BW, Putti TC, Dunn NR (2009) Teratoma formation by human embryonic stem cells: evaluation of essential parameters for future safety studies. *Stem Cell Res* 2(3):198–210. <https://doi.org/10.1016/j.scr.2009.02.002>
31. Zhang Y, Pak CH, Han Y, Ahlenius H, Zhang Z, Chanda S, Marro S, Patzke C et al (2013) Rapid single-step induction of functional neurons from human pluripotent stem cells. *Neuron* 78(5):785–798. <https://doi.org/10.1016/j.neuron.2013.05.029>
32. Muratore CR, Srikanth P, Callahan DG, Young-Pearse TL (2014) Comparison and optimization of hiPSC forebrain cortical differentiation protocols. *PLoS One* 9(8):e105807. <https://doi.org/10.1371/journal.pone.0105807>
33. Vierbuchen T, Ostermeier A, Pang ZP, Kokubu Y, Südhof TC, Wernig M (2010) Direct conversion of fibroblasts to functional neurons by defined factors. *Nature* 463(7284):1035–1041. <https://doi.org/10.1038/nature08797>
34. Gridina MM, Serov OL (2010) Bidirectional reprogramming of mouse embryonic stem cell/fibroblast hybrid cells is initiated at the heterokaryon stage. *Cell Tissue Res* 342(3):377–389. <https://doi.org/10.1007/s00441-010-1085-2>
35. Amps K, Andrews PW, Anyfantis G, Armstrong L, Avery S, Baharvand H, Baker J, Baker D et al (2011) Screening ethnically diverse human embryonic stem cells identifies a chromosome 20 minimal amplicon conferring growth advantage. *Nat Biotechnol* 29:1132–1144
36. Baker D, Hirst AJ, Gokhale PJ, Juarez MA, Williams S, Wheeler M, Bean K, Allison TF et al (2016) Detecting genetic mosaicism in cultures of human pluripotent stem cells. *Stem Cell Reports* 7(5):998–1012. <https://doi.org/10.1016/j.stemcr.2016.10.003>
37. Shimoda Y, Watanabe K (2009) Contactins: emerging key roles in the development and function of the nervous system. *Cell Adh* 3(1):64–70. <https://doi.org/10.4161/cam.3.1.7764>
38. Zuko A, Kleijer KTE, Oguro-Ando A, Kas MJH, van Daalen E, Zwaag B, Burbach JPH (2013) Contactins in the neurobiology of autism. *Eur J Pharmacol* 719(1-3):63–74. <https://doi.org/10.1016/j.ejphar.2013.07.016>
39. Koch P, Opitz T, Steinbeck JA, Ladewig J, Brüustle O (2009) A rosette-type, self-renewing human ES cell-derived neural stem cell with potential for in vitro instruction and synaptic integration. *Proc Natl Acad Sci USA* 106(9):3225–3230. <https://doi.org/10.1073/pnas.0808387106>
40. Chambers SM, Fasano CA, Papapetrou EP, Tomishima M, Sadelain M, Studer L (2009) Highly efficient neural conversion of human ES and iPSC cells by dual inhibition of SMAD signaling. *Nat Biotechnol* 27(3):275–280. <https://doi.org/10.1038/nbt.1529>
41. Yuan SH, Martin J, Elia J, Flippin J, Paramban RI, Hefferan MP, Vidal JG, Mu Y et al (2011) Cell-surface marker signatures for the isolation of neural stem cells, glia and neurons derived from human pluripotent stem cells. *PLoS One* 6(3):e17540. <https://doi.org/10.1371/journal.pone.0017540>
42. Kim D-S, Lee DR, Kim H-S, Yoo J-E, Jung SJ, Lim BY, Jang J, Kang H-C et al (2012) Highly pure and expandable PSA-NCAM-positive neural precursors from human ESC and iPSC derived neural rosettes. *PLoS One* 7(7):e39715. <https://doi.org/10.1371/journal.pone.0039715>
43. Gendrel AV, Attia M, Chen C-J, Diabangouaya P, Servant N, Barillot E, Heard E (2014) Developmental dynamics and disease potential of random monoallelic gene expression. *Develop Cell* 28(4):366–380. <https://doi.org/10.1016/j.devcel.2014.01.016>
44. Li SM, Valo Z, Wang J, Gao H, Bowers CW, Singer-Sam J (2012) Transcriptome-wide survey of mouse CNS-derived cells reveals monoallelic expression within novel gene families. *PLoS One* 7(2):e31751. <https://doi.org/10.1371/journal.pone.0031751>
45. Gimelbrant A, Hutchinson JN, Thompson BR, Chess A (2007) Widespread monoallelic expression on human autosomes. *Science* 318(5853):1136–1140. <https://doi.org/10.1126/science.1148910>
46. Xu J, Carter AC, Gendrel AV, Attia M, Loftus J, Greenleaf WJ, Tibshirani R, Heard E et al (2017) Landscape of monoallelic DNA accessibility in mouse embryonic stem cells and neural progenitor cells. *Nature Genet* 49(3):377–386. <https://doi.org/10.1038/ng.3769>